Status of LHCb

Giovanni Carboni

Dipartimento di Fisica, Università degli Studi di Roma "Tor Vergata"
and Sezione INFN Tor Vergata, Roma, Italy
On behalf of the LHCb collaboration

The status of the LHCb experiment is presented. The experiment has been taking data since the LHC startup. The performances of the various sub-detectors are discussed and a preliminary measurement of the $b\bar{b}$ cross-section is reported. The value is in agreement with expectations.

1. INTRODUCTION

The LHC machine has a unique potential for the study of CP violation and rare decays in the b sector due to the combination of a large $b\bar{b}$ production cross-section and high luminosity. Even at an average luminosity $\mathcal{L} = 2 \times 10^{32}$ cm^{-2}s^{-1}, well below the machine design value, 10^{12} $b\bar{b}$ pairs are produced per year, offering interesting perspectives in the quest for New Physics with an approach complementary to those of ATLAS and CMS [1].

LHCb is the only experiment at LHC designed to exploit this potential with an optimized detector, which incorporates precision vertexing and tracking systems, particle identification over a wide momentum spectrum and the capability to trigger down to very small transverse momenta. LHCb can work for years at constant luminosity, independently from the other intersections, thus collecting clean events of constant quality.

The results presented here correspond to the machine startup phase, with a reduced number of bunches and a value of $\sqrt{s} = 7$ TeV. The total integrated luminosity at the time of this conference (August 2010) amounts to 1 pb^{-1}. Using the data collected we show that the various subdetectors perform as planned. The $b\bar{b}$ production cross-section has been measured by two independent methods and confirms the expectations on the sensitivity for the experiment.

2. DETECTOR PERFORMANCE

A schematic drawing of the LHCb detector is shown in Fig. 1. It is a single-arm open spectrometer using a large dipole magnet (bending power 3.6 Tm) for momentum measurement. This geometry exploits the fact the $b\bar{b}$ production is peaked in the forward direction. The apparatus is described in detail in [2].

The LHCb detector is fully equipped since the startup of LHC, except for the online trigger and DAQ farm which is still under completion. The geometry of LHCb is not well suited to rely on cosmic rays for calibration purposes, therefore most of the calibration and alignment work has been performed with particles from beam-beam collisions but also using beam-dump and beam-gas interactions. The performances of the various subdetectors are summarized below.

Tracking. The tracking system comprises a silicon strip detector (VErtex LOcator or VELO) to reconstruct precisely the tracks close to the interaction region, followed by a larger silicon tracker before the magnet and by a hybrid tracker (silicon plus straw tubes) downstream of the magnet. The VELO is made of 21 silicon planes of semi-circular shape close to the collision point, orthogonal to the beam direction (along the z axis). The sensor strips are arranged to measure r and ϕ with a $10º - 20º$ stereo angle to improve spatial reconstruction. The VELO is mounted in a vacuum tank and the edges of the sensor planes are at few millimeters from the beam during data taking. They are retracted to ± 2.9 cm from the beam during machine injection. The alignment among sensors is better than 5 μm
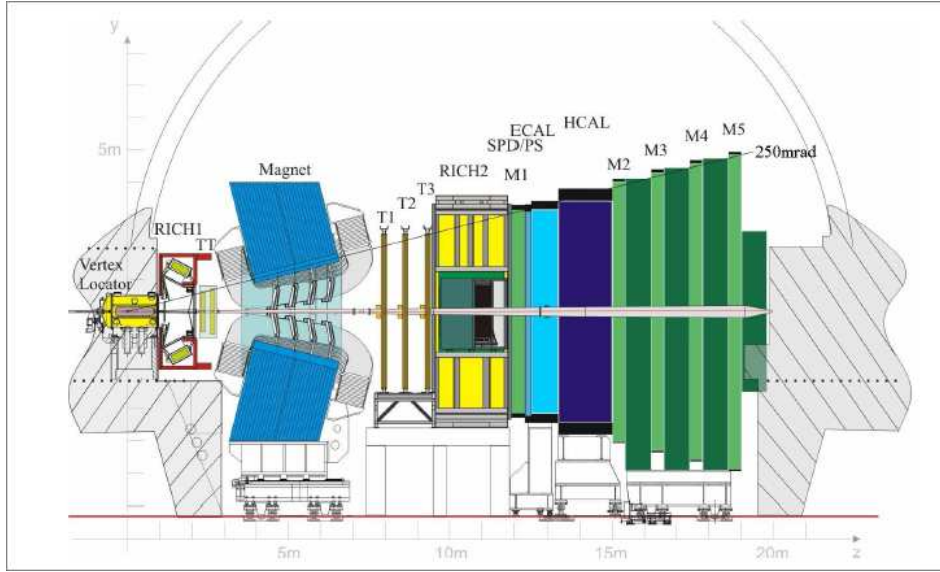
Figure 1: Schematic side view of the LHCb detector. RICH1 and RICH2: Ring Imaging Cherenkov; TT: Si Trigger Tracker; T1-T3: downstream tracker stations; SPD/PS: Preshower; ECAL and HCAL: calorimeters; M1-M5: Muon Stations. See text for additional details.

and the fill-to-fill variations are less than this value. This ensures excellent stability and hit resolution. The cluster finding efficiency is 99.7 % and the impact parameter resolution for high-momentum tracks is 16 μm to be compared with 11.2 μm from MC. Further improvement will be obtained by better alignment. The typical $z-$resolution for a primary vertex with 25 tracks is ≈ 90 μm. From the analysis of $b \to J/\psi$ decays a proper-time resolution of 60 fs has been obtained, giving excellent perspectives for time-dependent B_s CP violation studies.

Following the VELO is a large-area (1.4×2.1 m^2) silicon strip detector (TT or Trigger Tracker) upstream of the magnet. Downstream of the magnet there are three stations (T1 to T3) using silicon strips in the inner part (IT) and straw tubes on the outer part (OT). The hit resolution is ≈ 55 μm in the TT and IT and 250 μm in the OT straw tubes. Fig. 2 shows a typical K_S^0 mass peak as measured with or without the use of the VELO. The mass resolutions are already very good, and better alignment and calibration should allow the design values to be achieved, which is about 30 % smaller.
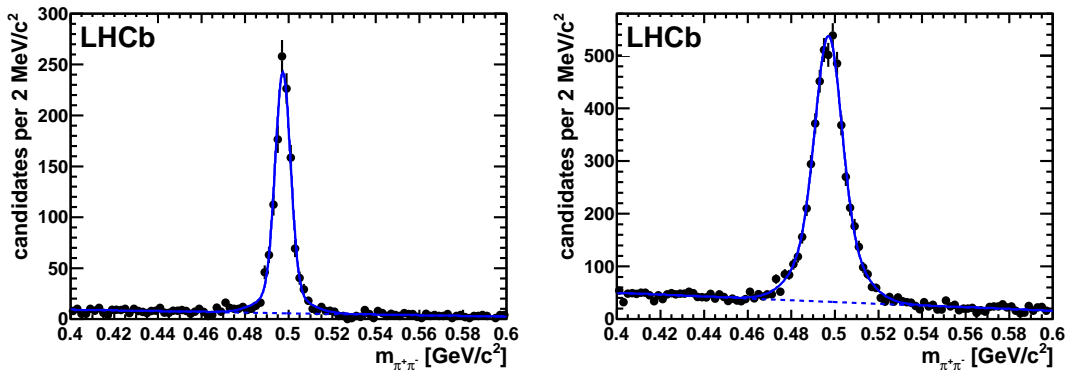

Figure 2: Tracking performance. Left: mass peak for K_S^0 mesons with both pion tracks detected in the VELO. Mass resolution is 5.5 MeV/c^2 Right: same for K_S^0 decaying after the VELO, with mass resolution 9.2 MeV/c^2 .

RICH. Two Ring Imaging Cherenkov detectors (RICH 1 and 2) with three radiators are used to identify charged particles in the momentum range $2-100$ GeV/c. They play a crucial role for the clean reconstruction of several important channels. RICH1 uses a silica Aerogel and a C_4F_{10} gas radiator, whereas RICH2 uses CF_4 gas. The

readout is via HPD pixel tubes. The angular resolution for the gas radiators (~ 2.2 and ~ 0.9 mrad respectively for RICH1 and RICH2) is close to the design values. A resolution larger than expected is obtained for Aerogel, partially due to gas contamination of the radiator, and work is ongoing to calibrate every single tile of the aerogel wall. The average efficiency for $K^{\pm}$ detection is about 95 % with a $\pi \to K$ misidentification probability of 7 %. Fig. 3 shows the effect of the RICH detectors in reconstructing three benchmark channels.
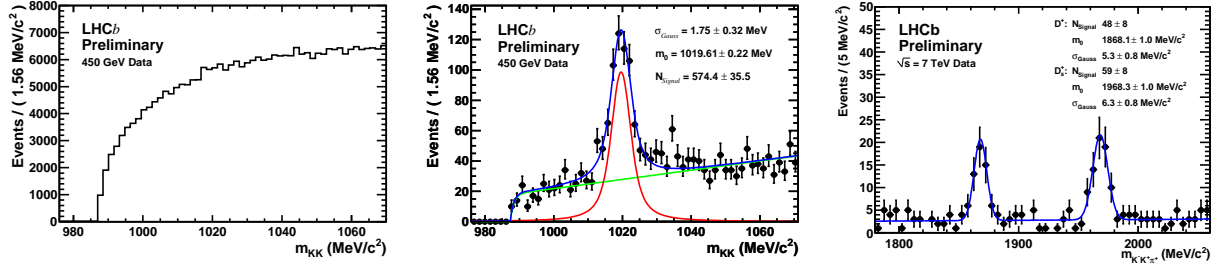

Figure 3: RICH performance. Invariant mass distribution for $\phi \to K^+K^-$ without (left) and with (center) K identification. For D^+ and D_s decaying to $K^+K^-\pi^+$ (right).

Calorimetry and Muon Detection. Level-0 (L0) triggering and particle identification of electrons, photons and muons are provided by dedicated subdetectors. The Hadron Calorimeter (HCAL), based on an iron/scintillator tiles design, is important for triggering on multi-hadron decays. In a typical case like *e.g.* $D^* \to D^0(K\pi)\pi$ the combined L0 and HLT (High level Trigger) efficiency is $60 \pm 4\%$, in good agreement with the Monte Carlo prediction (66 %).

For electrons and photons the Electromagnetic calorimeter (ECAL) and the PS/SPD Preshower detectors are used. The ECAL is a Shashlik-type sampling calorimeter, and its energy scale is calibrated to the 2 % level, yielding a resolution $\sigma_M = 7.2$ MeV/c^2 on the π^0 mass. Reconstruction of multi-body decays with one π^0 in the final state is particularly encouraging (Fig. 4).

The MUON System uses five stations, M1-M5, equipped with 1368 fast MWPC chambers supplemented by 24 Triple-GEM chambers in the small-angle region of the first Muon Station (M1). Since many interesting channels contain muons the performance of the muon trigger and of muon identification are particularly important. An average muon ID efficiency $\epsilon(\mu) = 97.3 \pm 1.2\%$ has been measured on data, with a misidentification probability for $\pi \to \mu$ around 2 % (see Fig. 4). The same figure shows the L0 trigger efficiency for $J/\psi \to \mu\mu$ events *vs.* J/ψ p_T. The average efficiency measured on data (96.1 ± 2.0 %) agrees with the Monte Carlo prediction.
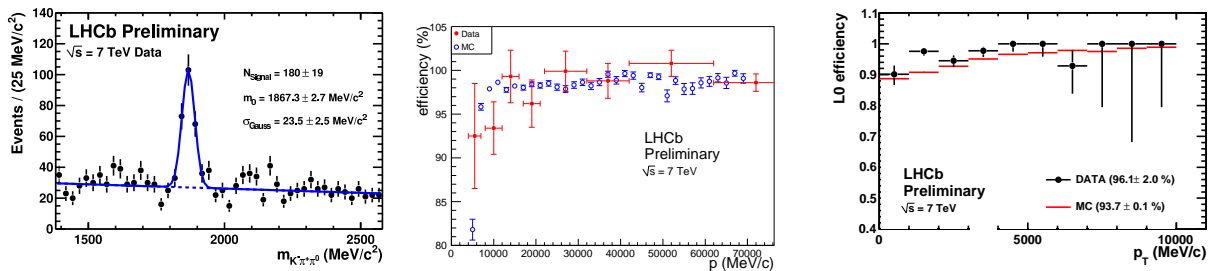

Figure 4: Left: $D^0 \to K^-\pi^+\pi^0$, with π^0 reconstructed by ECAL and PS. Center: muon ID efficiency *vs.* muon momentum. Right: L0 trigger efficiency for $J/\psi \to \mu\mu$ *vs.* J/ψ p_T.

Trigger architecture. The LHCb trigger is based on a powerful and very flexible multilevel architecture. Its task is extremely challenging since only $\sim 1/100$ of the events contain a $b\bar{b}$ and in addition the interesting channels have branching ratios smaller than 10^{-3}. At the lowest level (L0) the trigger is designed around dedicated electronics hardware operating synchronously with the 40 MHz bunch-crossing frequency and uses high-p_T particles in the CALO and MUON systems to reduce the data rate from the 40 MHz bunch crossing frequency to 1 MHz. The

entire detector can be readout at this frequency. The output of L0 is fed to the software High Level Trigger (HLT), running asynchronously on a computer farm that will have 14000 processor cores in its final phase. The HLT adds the informations from the tracking subdetectors (HLT1) and passes the interesting events for further analysis to HLT2. HLT2 has the capability of full event reconstruction to select the events to be written on tape at 2 kHz. In the present startup phase the demand on the trigger is very much reduced and therefore the HLT2 has been running in pass-through mode, and the selections cuts for p_T and impact parameter in L0 and HLT1 have been softened. The total efficiency for B decays is at present $\simeq 70$ % for hadronic modes, and > 90 % for leptonic modes. In addition the relaxed cuts yield a large efficiency for charm events.

3. b-PRODUCTION CROSS-SECTION RESULTS

The first data taken with the LHCb experiment at 7 TeV centre-of-mass energy have allowed the measurement of the $b(\bar{b})$ production cross-section in the LHCb acceptance. Beyond the intrinsic interest of this measurement, knowledge of the b yield is also critical in ascertaining the sensitivity of the LHCb experiment in flavour physics.

The preliminary measurements of σ_b presented in this paper correspond to an integrated luminosity $\int \mathcal{L}dt \approx 14$ nb^{-1} and have been obtained by two independent methods. The first method [4] uses the inclusive decay $b \to J/\psi X$. The second method [5] exploits the semileptonic channel $b \to D^0 \mu \nu X$, with $D^0 \to K^- \pi$ The analysis is briefly presented below.

3.1. $b \to J/\psi X$

For this study the sample of $J/\psi \to \mu\mu$ has been collected using the muon trigger, corresponding to an integrated luminosity $\int \mathcal{L}dt = 14.2$ nb^{-1}. Full details of the analysis are presented in [4]. The trigger selected events with at least one muon track with $p_T > 1.3$ GeV/c (HLT1). In the analysis selection cuts have been applied to the tracks and vertex quality. The efficiency of the cuts and of the trigger and the acceptance of the detector have been evaluated using the LHCb Monte Carlo. The acceptance for the J/ψ depends on its polarisation. The limited statistics does not allow yet for the measurement the polarisation parameter α, therefore the cross-section has a systematic uncertainty due to the unknown value of α. In Fig. 5 the measured differential cross-section $d\sigma/dp_T$ is therefore presented for three representative values of the polarisation parameter. The value integrated over the LHCb acceptance is

$$\sigma(\text{inclusive } J/\psi; p_T < 10 \text{ GeV}/c, 2.5 < y < 4) = 7.65 \pm 0.19 \pm 1.10^{+0.87}_{-1.27} \, \mu\text{b}$$

where the errors are, in the order, statistical and systematical, the last error stemming from the unknown polarisation.

To separate the J/ψ produced in b decays we use the pseudo proper time $t_z = d_z M/P_z$ where d_z is the projected distance bewteen the primary and the dimuon vertx, and M and P_z are the J/ψ mass and longitudinal momentum respectively. A plot of the t_z distribution is shown in Fig. 5. Fitting the exponential decay term yields the fraction of J/ψ from b decays, $f_b = 11.1 \pm 0.8$ % and a lifetime $\tau_b = 1.35 \pm 0.10$ ps. From this the cross-section for producing a J/ψ from b decay is obtained:

$$\sigma(J/\psi \text{ from } b; p_T < 10 \text{ GeV}/c, 2.5 < y < 4) = 0.81 \pm 0.06 \pm 0.13 \, \mu\text{b}$$

In this case, since many possible decay channels contribute to the J/ψ production, an effective zero polarisation was assumed. By extrapolating to the full solid angle using PYTHIA 6.4 [3] the total $b\bar{b}$ production cross-section takes the value $\sigma(b\bar{b}) = 319 \pm 24 \pm 59 \, \mu$b. This value is in good agreement with the extrapolation from Tevatron energies using PYTHIA with the colour-octet diagrams included.

3.2. $b \to D^0 \mu \nu X$

In this analysis the D^0 mesons from a parent b are separated from those directly produced on the basis of the impact parameter (IP) of the reconstructed D track measured with respect to the primary vertex. The D^0 is reconstructed
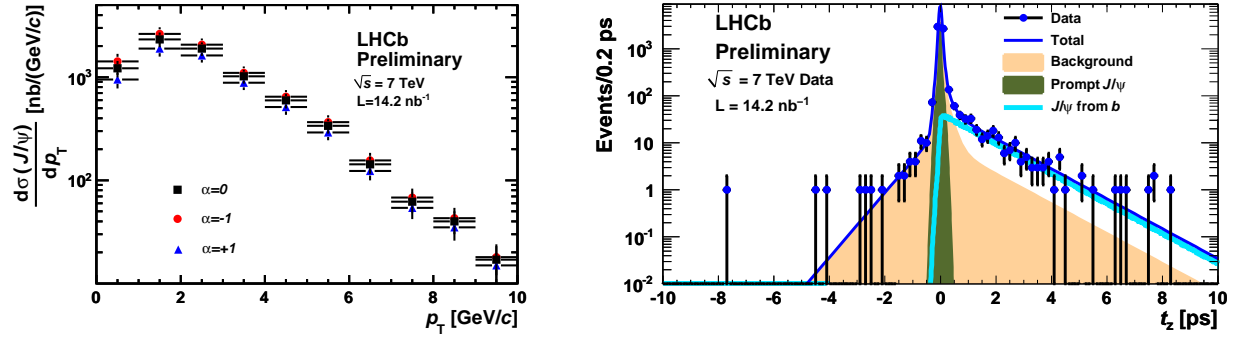
Figure 5: Left: $d\sigma/dp_T$ for inclusive J/ψ production, shown for three representative values of the J/ψ polarisation (in the helicity frame). Right: pseudo proper time (see text) distribution of the J/ψ events, showing the various contributions.

from the $K^-\pi^+$ decay. Full details of this analysis are reported in [5].

Two independent data samples, recorded at different times, were analyzed. A so-called *microbias* sample comprised events with a very loose trigger, requiring at least one track to be reconstructed in either the VELO or the tracking stations ($\int \mathcal{L}dt = 2.9$ nb^{-1}). The second sample, referred to as *triggered*, used triggers designed to select a single muon ($\int \mathcal{L}dt = 12.2$ nb^{-1}).The two samples were analyzed independently and the results combined.

The $D^0 \to K^-\pi^+$ candidates were matched with tracks identified as muons. Signal events from b must have the same the same sign of the muon and of the kaon (RS events). The opposite associations (WS) indicated a background event. The IP distributions of both RS and WS candidates, requiring that the $K^-\pi^+$ invariant mass is within 20 MeV/c^2 of the D^0 mass, are shown in Fig. 6 confirming that the WS events are highly suppressed.
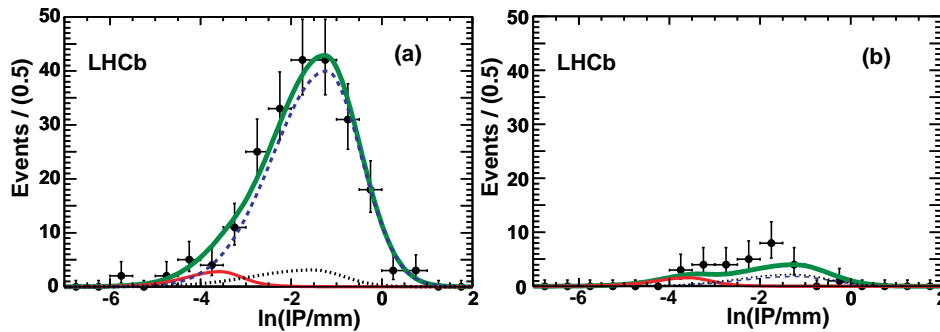

Figure 6: Natural logarithm of the D^0 IP in the 12.2 nb^{-1} triggered sample for (a) right-sign and (b) wrong-sign D^0-muon candidate combinations (see text). The dotted curves show the D^0 sideband backgrounds, the thin solid curves the Prompt yields, the dashed curve the signal, and the thick solid curves the totals.

Since the θ angle of the b hadron is obtained from the $D^0 - \mu$ vertex, it is possible to measure the differential cross-section $d\sigma_b/d\eta$. The results are reported in [5] together with the predictions of two theoretical calculations (MCFM [6] and FONLL [7]). Integrating over the LHCb pseudorapidity acceptance yields the value

$$\sigma_b(pp \to H_bX; 2 < \eta_b < 6) = 75.3 \pm 5.4 \pm 13 \ \mu\text{b}$$

Extrapolating to the full solid-angle using again PYTHIA 6.4 [3] yields the value $\sigma(b\bar{b}) = 284 \pm 20 \pm 49 \ \mu\text{b}$, in good agreement with the value obtained from the $b \to J/\psi$ mode.

Proceedings of HCP2010 – Toronto

4. CONCLUSIONS

The LHCb experiment is in excellent shape. More than 99 % of the various sub-detectors are operational, and perform very close to the expectations. Work is in progress to refine further the alignments and calibrations. The b-production cross-section has been measured in two different channels. Combining the two measurements corresponds to a total $b\bar{b}$ production cross-section

$$\sigma(b\bar{b}; \sqrt{s} = 7 \text{ TeV}) = 298 \pm 15 \pm 43 \, \mu\text{b} \qquad \text{(weighted average of two measurements)}$$

This value agrees with the expectations and confirms that the b yield assumed in the design of LHCb was correct. With reasonable assumptions on the integrated luminosity of the 2010-2011 run LHCb will be able to carry on its physics program and access signatures sensitive to possible New Physics in CP violation and rare decays.

References

1 F. Teubert, these proceedings.

2 A. Augusto Alves Jr. et al., (LHCb Collab.) "The LHCb Detector at the LHC" JINST 3 (2008) S08005.

3 T. Sjöstrand, S. Mrenna and P. Skands, "PYTHIA 6.4: Physics and manual", JHEP **05** (2006) 026.

4 LHCb Collaboration, Conference Note CERN-LHCb-CONF-2010-010 (2010).

5 LHCb Collaboration: E. Aaij et al., arXiv:1009.2731v1 (2010), to be published in Physics Letters B.

6 The MCFM version 5.8 computer program was used to evaluate the $b\bar{b}$ production cross-section. See J. M. Campbell and K. Ellis "MCFM - Monte Carlo for FeMtobarn processes", at http://mcfm.fnal.gov/ and references therein.

7 Private communication from M. Cacciari, P. Nason, S. Frixione, M. Mangano, and G. Ridolfi. See also M. Cacciari, S. Frixione, M. L. Mangano, P. Nason and G. Ridolfi, JHEP 0407 (2004) 33; M. Cacciari, M. Greco and P. Nason, JHEP **9805** (1998) 007.